Strain investigations on calcite marbles using neutron time-of-flight diffraction

C. Scheffzük · S. Siegesmund · A. Koch

Abstract In order to describe and explain the effect of bowing of marble facade panels, neutron time-of-flight diffraction was applied to determine residual macro- and microstrain on the calcite mineral phase. The measurements were combined with investigations of the crystallographic preferred orientation (texture) measurements by neutron diffraction, macroscopic measuring of the bowing on marble building stones, as well as microfabric analyses. Three samples were investigated to explain the bowing effect: a fresh broken sample, a good conditioned facade panel and a strongly deformed facade panel. Residual intracrystalline strain was detected in all investigated samples, which differed in the degree of bowing. For the first time, the preferred orientation and the residual strain were found to be related. The results show that different strain magnitudes are reflected by residual strains, which differ significantly in magnitude and direction. Furthermore, different Bragg peak widths have been detected as an indication of microscopic strain. The observed residual strain values in the samples are related with the grain shape and texture properties.

Keywords Calcite · Marble · Neutron diffraction · Strain and stress · Texture

Published online: 4 June 2004

C. Scheffzük (✉)
GeoForschungsZentrum Potsdam (Section 5.3),
Telegrafenberg, 14473 Potsdam, Germany
E-mail: scheff@gfz-potsdam.de
Tel.: +49-331-2881167
Fax: +49-331-2881127

C. Scheffzük
Frank Laboratory of Neutron Physics, Joint Institute for Nuclear Research Dubna, 141980 Dubna, Russia

S. Siegesmund · A. Koch
Department of Structural Geology and Geodynamics, Geoscience Centre of the University of Göttingen, Goldschmidtstr. 3, 37077 Göttingen, Germany

Introduction

Durability is an important issue to consider when specifying the stone for exterior exposure. However, many marbles have shown a bowing of facade panels after a short period of exposure. This bowing is generally accompanied by the reduction of strength properties as the degree of bowing increases (e.g. Logan and others 1993; Mustonen 1993; Koch and Siegesmund 2002). Well-known examples of completely destroyed facade claddings are those from the Finlandia Hall in Helsinki (Ritter 1992), the Amoco building in Chicago (Logan and others 1993), and the Grand Arche de la Defense in Paris. All of them are made of Carrara marble. Kessler (1919) and Rayleigh (1934) found that the bowing took place due to repeated heating, which could result in permanent dilatation. Thermal heating (e.g. Franzini 1995 or Widhalm and others 1996) and cooling (Ondrasina and others 2002) are supposed to be an important factor for these observed deterioration phenomena. In a more systematic study, Siegesmund and others (2000) as well as Zeisig and others (2002) showed that, with respect to heating and cooling, four distinct groups of marbles may be distinguished. Moreover, it was proposed that the degree in bowing may be related to the rock fabric, i.e. the lattice and shape-preferred orientation and pre-existing microcracks (see also Koch and Siegesmund 2004). Recently, these observations have been modified by microstructure-based finite-element simulations by Weiss and others (2002, 2003). Bortz and others (1988) and Winkler (1994) emphasised the importance of moisture and concluded that any variation in moisture contents may cause deformation. Continuous rows of ordered water molecules oriented on both sides of the capillary wall may cause swelling by elongation and marble disruption (Winkler 1994). Logan and others (1993) and Logan (2004) explain the bowing of thin marble slabs by the anomalous expansion-contraction behaviour of crystalline marble and the release of locked-in residual stresses.

Residual stresses of the first and second order can be assessed by means of X-ray or neutron diffraction. X-ray diffraction method was already applied by Reik (1976) to investigate residual stresses on rocks. But in the last few years neutron diffraction method has been also applied on geomaterials, such as quartz (Scheffzük and others 1998; Walther and others 1998), dolomite (Scheffzük and others

 DOI 10.1007/s00254-004-1048-6

2001) and a shock deformed quartz-dunite compound (Walther and others 2004). Furthermore, external load experiments on sandstone were carried out to investigate the effect of applied stresses using conventional neutron diffraction and time-of-flight neutron diffraction (Frischbutter and others 2000). Applied experimental equipment is described by Walther and others (2000) and Frischbutter and others (2002).

Residual microstresses are preserved in any plastically deformed rock and depend upon the elastic and thermal properties of the constituents and on the lattice orientations. To quantify residual strain, marble panels from the 'Oeconomicum' building of the University campus at Göttingen (Germany) were demounted and investigated (Nordtest Method 2002). Koch and Siegesmund (2002) measured the bowing of the marble panels systematically and found a relationship between the rock fabric and the degree of bowing. This paper describes first results of the experiments obtained from selected panels and analysed by intracrystalline strain measurements applying neutron time-of-flight diffraction. The results were compared to an undeformed fresh broken sample from the same material to check whether the locked-in stress might be also a controlling factor of marble bowing.

The Oeconomicum building

The three-stored 'Oeconomicum' building at the University of Göttingen was built in 1966 (Fig. 1a). All facades are clad with panels of a white to dark, strongly decorated Peccia marble of identical dimensions. Most of the panels exhibit remarkable concave (inwards) bowing (Fig. 1b). The frequency of visible damages, such as cracks (Fig. 1c) and breakouts, increases with the degree of bowing. The degree of bowing is different at each facade and each panel row (Fig. 2). Nearly all panels are bent concavely except for the east facade where row 2 shows a clear convex bowing of about (-6.8 ± 2.3) mm/m. The maximum row average in concave bowing can be observed at the east facade as well, where the uppermost row 4 displays a mean value of (15.6 ± 2.9) mm/m. The maximum value for a single panel was also recorded in the uppermost row (23 mm/m). In contrast, the west, south and north facades exhibit a more homogeneous distribution with a low mean concave bowing in the lowermost rows (0.9–3.7) mm/m and an intermediate degree of bowing in rows 2–4 with mean values of (6–10) mm/m at the west and south facades, and (3–5) mm/m at the north facade.

All panels were combined into groups of four except the outermost ones (see Fig. 1a). Rarely, the bowing is different from panel to panel within a single group, but rather from one group to the next group. Connected therewith is the macroscopically observed structure, which is comparable for each single panel within each group of four panels and different between the groups. This means that the cutting direction was different with respect to any metamorphic layering, foliation or macroscopic folds for most of the groups. For aesthetic reasons the panels with identical ornamental or decorative elements, i.e. the same cutting direction, were combined.

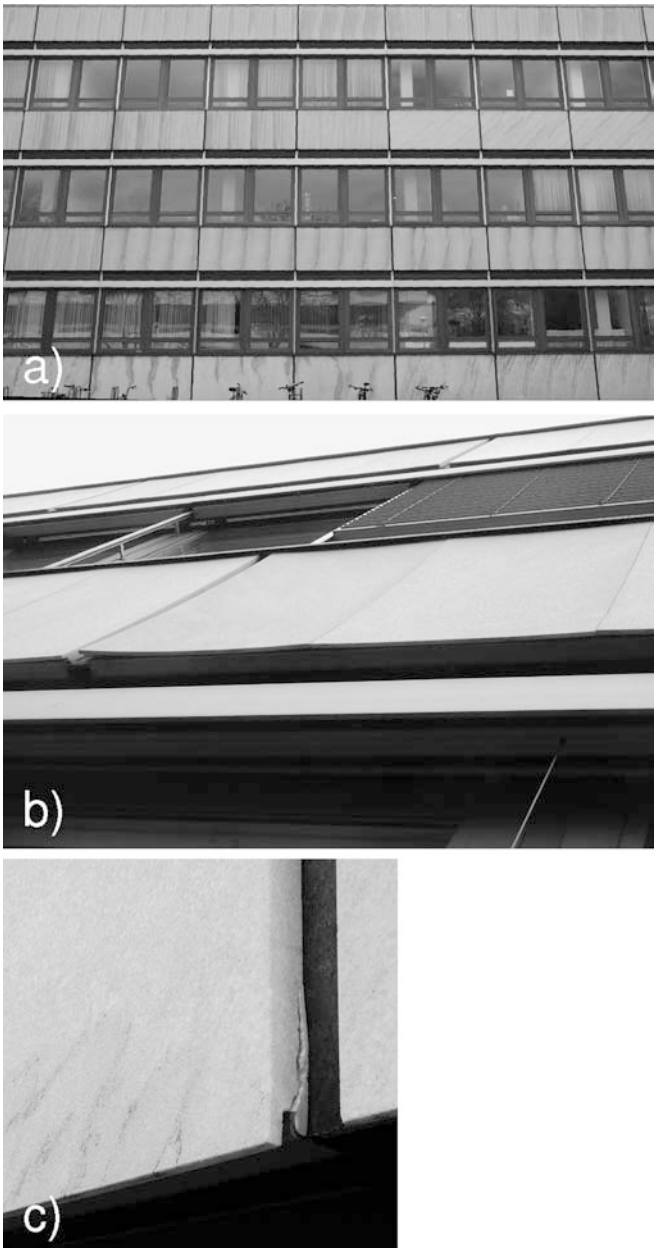

Fig. 1
a) Representative part of the Oeconomicum building in Göttingen (western part, north facade). Observed damage on the investigated marble panels: **b**) concave bowing (*left panel*) and **c** crack at the lower corner

Experimental

Strain investigations were carried out on marble samples of (100×100×30) mm applying neutron time-of-flight diffraction at the pulsed neutron source IBR-2 at JINR, Dubna (Fig. 3). The neutron pulse covers the wavelength

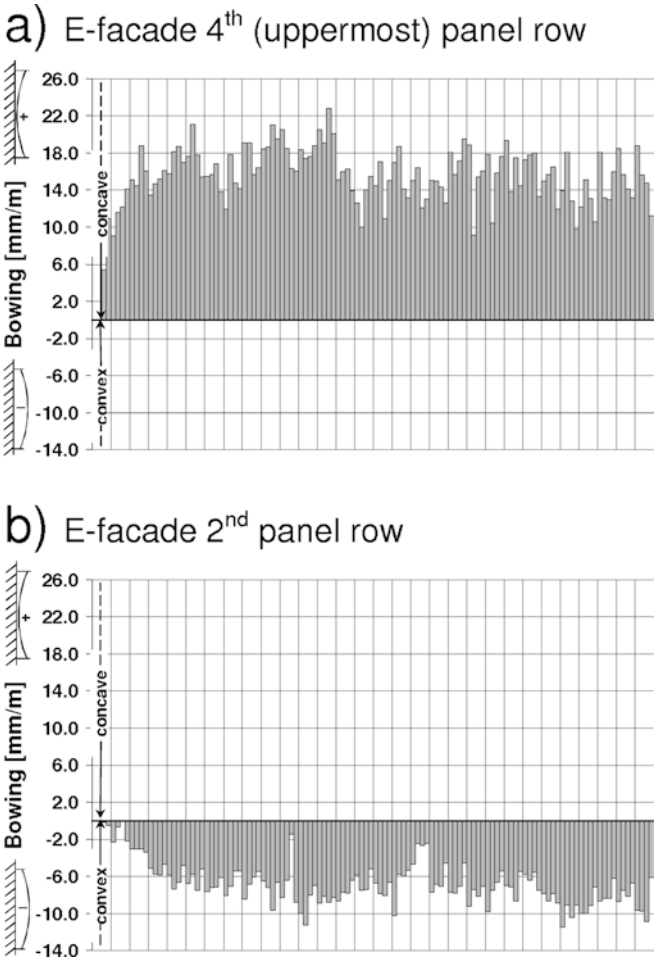

Fig. 2
Quantification of the bowing of selected facade panels of the east facade: **a**) 4th (uppermost) panel row: concave bowing; **b**) 2nd panel row: convex bowing

range from 0.8 to 7.6 Å. The long flight path of 101.26 m allows one to detect all Bragg reflections in the range of lattice spacings from 0.6 to 5.3 Å, simultaneously.
The EPSILON-MDS diffractometer is a multi-detector-system including a four-axes goniometer, which provides rotation about one axis and translation in three perpendicular directions. High precision sample positioning is guaranteed by means of step motors. Furthermore, the diffractometer consists of nine radial collimators equipped with single ^{3}He counter tubes, 10 mm in diameter and 200 mm long. The nine collimator-detector units are arranged at angles of −21°, 0°, 21°, 69°, 90°, 111°, 159°, 180° and 201° around the incident beam and cover the 2Θ-range of 82°< 2Θ< 98° (Walther and others 2000). Up to nine ^{3}He detectors are arranged at each collimator, one detector at each collimator is arranged at 2Θ=90°, the others are positioned at angles smaller or larger than 2Θ=90°. This increases the sample–detector distance. To sum up the spectra of all the detectors of any collimator, electronic time focusing was applied: the channel width of the electronic time analyser is adapted for each detector in dependence on 2Θ. The arrangement of nine collimators provides simultaneous recording of nine sample directions. Detector unit 2 is opposite to detector unit 8, by this, two sample directions perpendicular to each other may be considered (Fig. 3a). The spectral resolution $\Delta d/d$ is about $4\text{x}10^{-3}$ at d=2 Å. The available beam cross section of about (50×85) mm^{2}allows one to investigate large samples or to measure strain profiles. Based on these properties, the diffractometer EPSILON-MDS is well-suited for strain/stress investigation of polymineralic rocks consisting of low symmetrical phases (Frischbutter and others 2002).

Results

Samples

Three building stone samples made from calcite marble have been investigated: a fresh broken sample (P1), a good conditioned facade panel (P2) and a strongly deformed facade panel (P3). The microfabrics of the three samples have been examined by optical microscopy. The marbles are characterised by a broad grain-size distribution from medium to coarse grained: the average grain size is about 1 to 2 mm, the maximum grain size approximate 6 mm. Domains of coarser grain size exhibit polygonal to interlobate grain shape, and straight to slightly curved grain boundaries (Fig. 4). Domains of smaller grain size show interlobate to sometimes amoeboid grain boundary geometry, bulging occurs frequently, i.e. grain boundary migration is supposed to be the predominant mechanism of plastic deformation. More evidence of crystal–plastic deformation is indicated by deformation twins and undulous extinction. Furthermore, the fabric is characterised by grain boundary preferred orientation more or less parallel to the foliation plane (Fig. 4). In thin sections from strongly bowed panels, open grain boundaries, building intergranular microcracks, can be observed. The spacing of open cracks is up to 0.5 mm, their length is up to 5 mm (Fig. 4b). Intracrystalline cracks along twin planes are scarce. Apparently, there is a correlation between microcracks and bowing. The undeformed sample does not show any evidence of open grain boundaries in contrast to the strongly deformed sample. For P2, a warping of 0.2 mm/m has been measured, whereas for sample P3 a warping of 17.1 mm/m has been observed.

Textures

The fresh broken Peccia marble sample (P1) was measured via neutron time-of-flight diffraction at the SKAT texture diffractometer at the IBR-2 in Dubna. The instrumental characteristics are described by Ullemeyer and others (1998). The sample exhibits a strong crystallographic preferred orientation (texture; Fig. 5). The (0006) pole figure of calcite shows an intensity maximum normal to the macroscopic foliation with a weak tendency to form a girdle distribution around an *a*-axis maximum lying in the foliation plane. The tendency of the $(11\bar{2}0)$ poles to form a great circle around the (0006) pole maximum (Fig. 5) is well-pronounced. The importance of calcite textures for the physical weathering of marbles has been widely

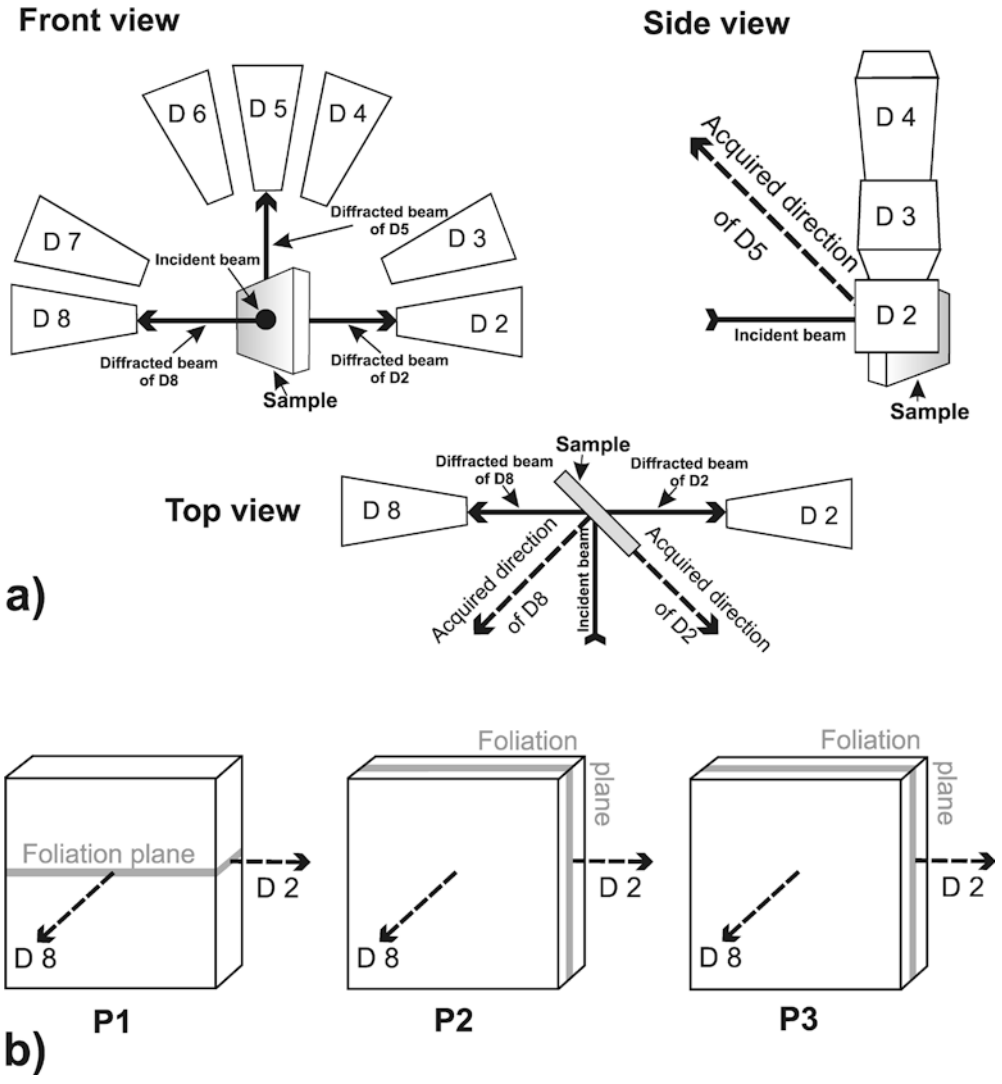

Fig. 3
Sketch of the experimental set-up **a**) for strain measurements with neutron diffraction and **b**) presentation of the measuring direction. The measuring directions are also given with respect to the macroscopic fabric elements as schematic sample cuboids

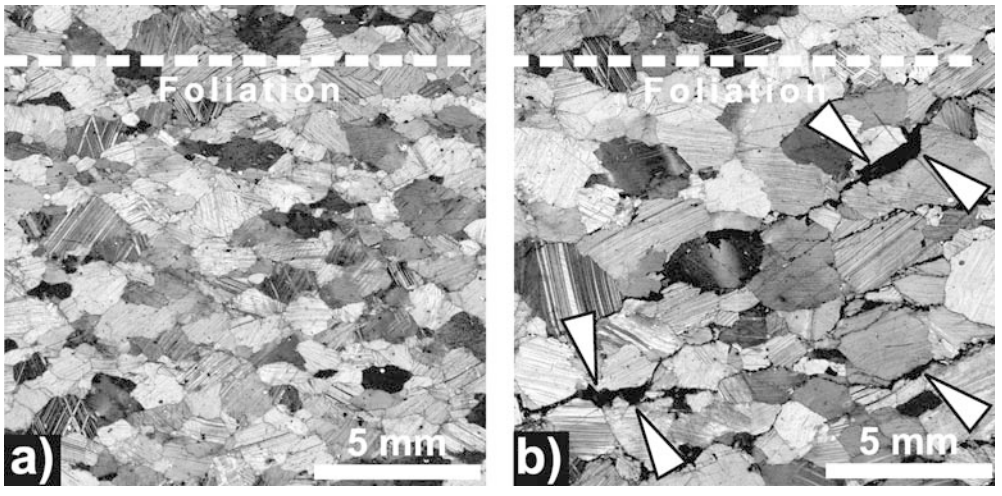

Fig. 4
Thin section images from demounted panels: **a**) Section vertical to foliation (weak bowing of the good conditioned panel P2). **b**) Section vertical to the foliation plane (strong bowing of the strongly deformed panel P3). The open grain boundaries are indicated by *arrows*

discussed. The general observation is that the direction of maximum deterioration is closely related to the *c*-axis maximum. This paper shows only the texture of the fresh broken sample (P1) because the textures of the good conditioned plate (P2) and the strongly deformed facade plate (P3) turned out to be similar.

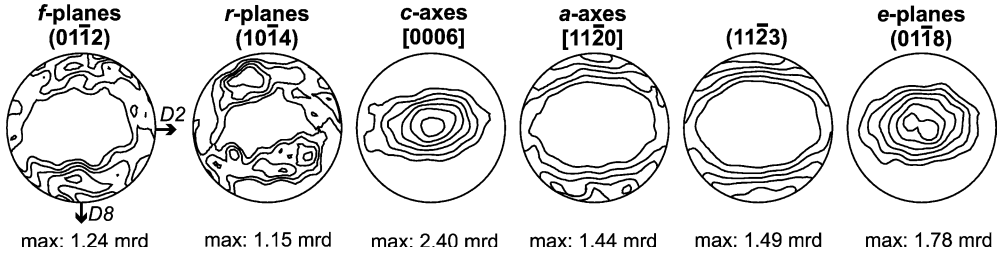

Fig. 5
Crystallographic preferred orientation of the fresh broken Peccia marble (sample P1), measured by neutron time-of-flight diffraction. Lower hemisphere; equal area projection onto the foliation plane; lowest contour level is one time random distribution; maximum intensities are indicated

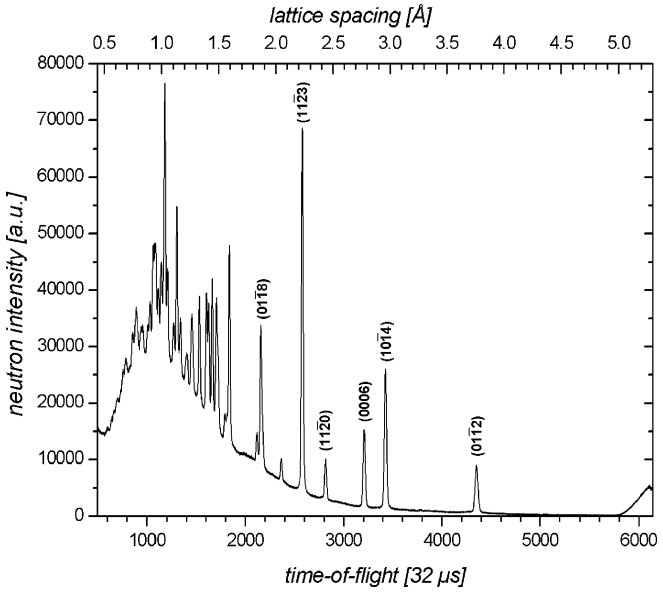

Fig. 6
Neutron time-of-flight diffraction pattern of the calcite sample P1, measured at the strain/stress diffractometer EPSILON-MDS at the pulsed neutron source IBR-2 in Dubna (Russia)

Residual stresses

Six Bragg reflections of calcite (01$\bar{1}$2), (10$\bar{1}$4), (0006), (11$\bar{2}$0), (11$\bar{2}$3)and (01$\bar{1}$8)(referred to hexagonal indices) have been investigated with respect to residual stresses (Fig. 6). Macroscopic internal stresses ($\varepsilon = \Delta d/d$) of all samples have been determined by analysing the position of the Bragg peaks in relation to the stress-free state (Fig. 7). The stress-free reference value has been determined by measuring rock powder, prepared by grinding down to a grain size of 200 μm and 24 h annealing at a temperature of 600 °C. Microscopic internal stresses caused by dislocations and other microscopic defects are caused by Bragg peak broadening (Fig. 7). The graphs indicate the interdependence of macroscopic and microscopic strains on particular Bragg reflections, i.e. lattice spacings. Regarding the experimental geometry of the neutron diffraction experiment, the detector units 2 and 8 were detecting two directions oriented perpendicular to each other, so that the most valuable directions parallel and perpendicular to the foliation plane could be recorded simultaneously.

A positive strain (residual tension) ε=(150±90)x10^{-6} has been detected in the acquired direction of detector unit 2 for the *f*-(01$\bar{1}$2)-planes of the strongly deformed facade panel (P3), whereas the fresh broken sample (P1) has shown a negative strain (residual compression) of ε= (–120±80)x10^{-6}. The good conditioned facade panel (P2) shows compressive strain of ε=(−180±70)x10^{-6}. For the *r*-planes ((10$\bar{1}$4) Bragg reflection) and the *e*-planes ((01$\bar{1}$8)Bragg reflection), the strongly deformed sample (P3) has shown contraction of $\varepsilon_{(10\bar{1}4)} = (-397 \pm 117) \times 10^{-6}$ and $\varepsilon_{(01\bar{1}8)} = (-240 \pm 200) \times 10^{-6}$ in contrast to a nearly strain-free state measured in the fresh broken (P1) and in the good conditioned sample (P2). The *c*-axes [(0006) Bragg reflection] are characterised by negative (tensional) strain: the fresh broken sample by (–250 ± 120)x10^{-6}, the good conditioned facade panel by (−170 ± 160)x10^{-6}, the strongly deformed facade panel by (−120 ± 120)x10^{-6}. All samples have shown nearly strain-free values for the *a*-axes ((11$\bar{2}$0) Bragg reflection) and for the (11$\bar{2}$3)Bragg reflection. Furthermore, all the samples show comparable macroscopic strains for the *c*-[0006]-axis, the *a*[{11$\bar{2}$0] – axis, the (11$\bar{2}$3)Bragg reflections and the *e*-planes (01$\bar{1}$8), with a tendency to contraction in the strongly deformed facade panel. Microscopic strain by peak broadening has been found at the strongly deformed facade panel (P3) on the *a*[{11$\bar{2}$0] – axis with a full width at half maximum (FWHM) of (21.8±1.0) time channels * 32 μs in relation to a FWHM of (17.8±0.3) time channels * 32 μs for the fresh broken sample and the good conditioned facade panel.

Positive (tensional) strain of the *f*-planes ((01$\bar{1}$2)Bragg reflection) has been detected in the acquired direction of detector unit 8 for all samples. At the strongly deformed facade panel (P3) a positive strain (tension) ε of about (780±130)x10^{-6} has been recorded, whereas the fresh broken sample (P1) has shown the maximum strain value of ε=(950±110)x10^{-6}. The good conditioned facade panel (P2) has also shown positive strain (tension) of ε=(400±210)x10^{-6}. The microscopic strain magnitudes show no significant differences between the three samples investigated. Only the experimentally produced reference powder shows considerable peak broadening. This may be caused by preparation, i.e. internal microscopic stresses were produced by the generation of a large number of dislocations by grinding. Note, that thermal treatment did not influence the dislocation density.

For the *r*-planes ((10$\bar{1}$4)-Bragg reflection) only the good conditioned and strongly deformed facade panels shown positive strain (tension), whereas the fresh broken facade panel displays the negative strain (compression). The good conditioned sample shows the positive strain (tension) of

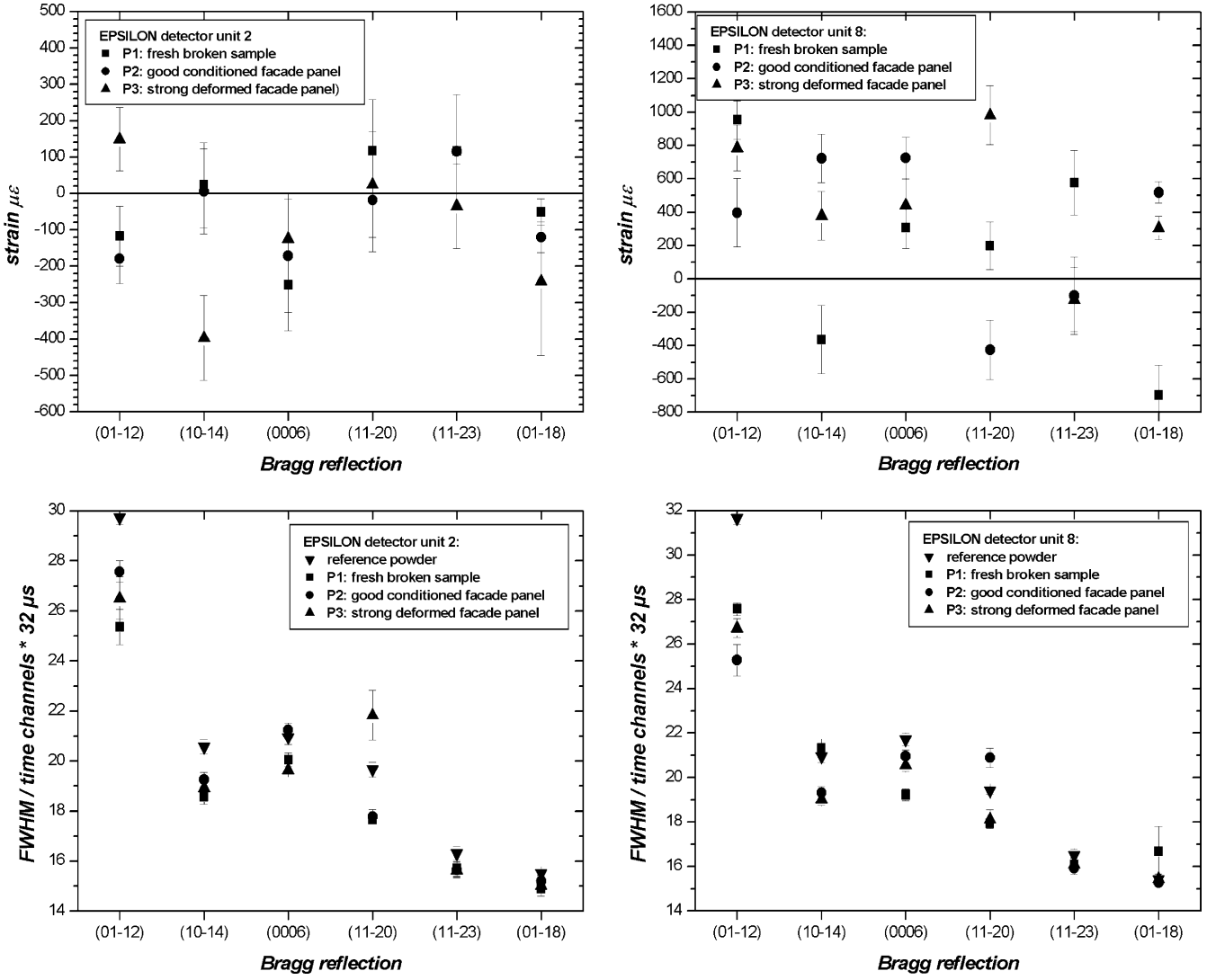

Fig. 7
Macrostresses **top**: determined from Bragg peak position in relation to the stress-free rock powder and **bottom**: microstresses calculated from the full width at half maximum (FWHM) in comparison to the reference rock powder

ε=(720±150)x10^{-6}, the strongly deformed facade panel tensional strain of ε=(380±140)x10^{-6}. In contrast, the *r*-planes of the fresh broken sample are characterised by negative strain (compression) of about ε =(−360±200)x 10^{-6}. All three panels display comparable macroscopic positive strain for the *c*-axis [0006]: the maximum value recorded at the good conditioned facade panel is ε=(720±120)x10^{-6}, the strongly deformed facade panel shows a magnitude of ε =(440±160)x10^{-6}, the fresh broken sample of ε=(300±120)x10^{-6}. The microscopic strain is characterised by lower FWHM for the fresh broken sample [(19.2±0.3) time channels * 32 μs] in contrast to somewhat larger FWHM for the good conditioned and strongly deformed samples [(21.0±0.3) and (21.6±0.3) time channels * 32 μs], respectively. The $a[\{11\bar{2}0] -$ axes are characterised by highest positive strain value at the strongly deformed facade panel of ε=(980±170)x10^{-6}. The fresh broken sample shows tensional strain of ε=(200±140)x10^{-6}, whereas the good conditioned facade panel shows negative compressive strain of ε=(−420±180)x10^{-6}. For the $(11\bar{2}3)$Bragg reflection the good conditioned and strongly deformed facade panels have demonstrated similar small compressive strain values of about ε=(−100±200)x10^{-6}. Only the fresh broken sample shows the tensional strain of ε=(577±193)x10^{-6}. The microscopic strain magnitudes are nearly the same with a FWHM of about 16 time channels * 32 μs. Concerning the fresh broken sample, the *e*-planes $((01\bar{1}8)$Bragg reflection) show compressive strain of about ε=(699±180)x10^{-6}, both the other samples are characterised by comparable tensional strain of ε =(518±64)x10^{-6}(P2) and ε=(305±69)x10^{-6} (P3). In relation to the good conditioned and strongly deformed samples the fresh broken sample has demonstrated somewhat larger FWHM.

Discussion and conclusion

Logan and others (1993) and Logan (2004) explained the bowing of thin marble slabs on the Amoco Building in Chicago by anomalous expansion–contraction behaviour

of calcite combined with the release of locked-in residual stresses. Logan's key observations are based on careful tests where marble panels are cyclically heated and cooled, leading to granular decohesion and strength losses. After 214 h the differential strain measurements on overcored thin marble panels have shown, on average, 20 to 85 microstrains, up to 900 microstrains at maximum. However, it seems to be not so easy to separate the strain fraction caused by the geological history from that stored during heating and cooling cycles, which may produce significant loss of decohesion at the grain boundaries. The degree in grain boundary damage is documented in the microstructures of the fresh (P1) and strongly deformed samples (P3), whereas the good conditioned sample (P2) represents an intermediate stage. As it has already been discussed in the literature (e.g. Kessler 1919; Rayleigh 1934; Sage 1988; Franzini 1995; Widhalm and others 1996; Siegesmund and others 2000; Zeisig and others 2002), the initial stage of physical weathering is most probably caused by the anisotropic single crystal elastic properties of calcite crystals. Based on finite element modelling, Weiss and others (2003) have already shown quantitatively that the crystallographic preferred orientation (texture) of calcite leads to directional dependence of the thermal expansion coefficient, and to permanent length changes. Moreover, Weiss and others (2003) have clearly demonstrated that weak calcite textures (for example Carrara marble) possess higher residual strains compared to marbles with strong textures (e.g. Peccia marble).

In the case of the Peccia marble this means that the metamorphic overprint and long-lasting deformation events were stored. Residual stress exists in a rock, even if the rock is not loaded externally. It is composed of two parts: (1) crystal distortions, reflecting previous external load locked in the aggregate, called locked-in stress, and (2) those that constrain them, called locking stress (for discussion see Friedman 1972, Hoskin and Russel 1981). In sedimentary rocks such as sandstone the development of residual stresses was discussed by Friedman (1972) and modelled by Reik and Vardar (1974). Dry sand gets deeply buried, the sand grains get squeezed together by the weight of overburden, and finally get strained elastically. At a later stage, the unstrained cement precipitates and locks the grains together forming sandstone. If unroofing later exposes the grains, the cement of the sandstone expands differently by causing stresses. However, these models do not explain residual stresses in magmatic and metamorphic rocks. Savage (1978) and Vollbrecht and others (1991) found that residual stresses in granitoids may be caused by thermal stresses resulting from different thermal contraction of quartz aggregates compared to the surrounding feldspar/mica framework during cooling and uplift. Savage (1978) considered the granitic pluton as a special inclusion within the infinite country rock, because cooling leads to different elastic strains since radial and tangential stresses are evident. Consequently, the superposition of two stress states, tectonic and thermal, occurs during cooling and solidification. Thermoelastic stresses can significantly exceed tectonic stresses. According to Timoshenko and Goodier (1970), the maximum horizontal thermoelastic stress (σ_T) can be calculated by:

$$\sigma_T = \alpha\, E\, \Delta T/(1-\nu) \qquad (1)$$

where α is the thermal expansion coefficient, E is the Young's modulus, ΔT is the temperature difference and ν is the Poisson's ratio. Assuming a cooling rate of 150 K per hour, the thermoelastic stress is about 42 MPa (α=7×10^{-6} K^{-1}, E =30 GPa and ν=0.25). In the case of metamorphic rocks, any explanation or hypothesis on residual locked-in stresses is still lacking, except that pressure solution (Emery 1964) or folding (Voight 1966) may produce significant residual stresses. As already discussed, the Peccia marble is strongly deformed and folded. The metamorphic conditions are estimated at a minimum of 400 °C due to the occurrence of biotite. In contrast to granitoids, marbles very often exhibit a strong crystallographic preferred orientation of the rock constituents. Moreover, calcite shows an extreme directional dependence of α at different crystallographic directions. (parallel <c>: α = 26×10^{-6} K^{-1}, perpendicular <c>: α = -6x10^{-6} K^{-1}, Kleber 1990). In contrast to quartz-rich rocks with its extreme volume expansion coefficient of about 37×10^{-6} K^{-1}, the extraordinary thermal expansion results in a relatively small volume expansion of around 6.6×10^{-6} K^{-1}. As a result of the strong calcite texture (Fig. 5) distinct elongation parallel to the *c*-axis maximum and a more or less neutral behaviour parallel to the *a*-axis maximum can be observed (Siegesmund and others 2000; Zeisig and others 2002). Applying Eq. (1) of Timoshenko and Goodier (1970) a maximum horizontal thermoelastic stress between −81.4 and 201 MPa for a temperature difference of 100 K can be expected. For the thermal expansion coefficient, the abovementioned maximum and minimum values as well as the Young's modulus ($E_{a\text{-}axis}$ =87.8 GPa and $E_{c\text{-}axis}$ =57.6 GPa) have been used because the anisotropic single crystal properties together with the preferred crystallographic orientation may significantly influence the thermoelastic properties. Already, Winkler (1994) mentioned that prestressed crystalline marble tends to expand more during the first cycle of heating as the locked-in stresses are released.

The measured Bragg peak positions are influenced by macro- and microstresses. Separate determination and interpretation of macrostresses is not possible because so-called microstresses should not be ignored, as diffraction methods like neutron stress analysis have never directly given macrostresses, but only a superposition of macro- and microstresses (Pintschovius 1992). Microstresses lead to broadening of Bragg diffraction lines. The broadening may arise from a number of factors, in particular, small crystal size, dislocations and stacking faults in the crystal structure, and variation of the lattice parameter in the microscopic scale due to internal strains or fluctuations in composition. Significant microstresses have been found in the acquired direction perpendicular to the foliation plane in the strongly deformed facade plate by a considerable peak broadening.

Gross and Paterson (1965) reported slight broadening of X-ray powder diffraction lines of deformed marbles when compared to the annealed ones. Peak broadening was attributed mainly to internal strains because, during annealing at temperatures above 400 °C, the peak broadening was reversed in two stages. In conclusion, they favoured the hypothesis that peak broadening may survive 'geological times' without complete removal by recovery and recrystallisation.

Since residual strain investigations are very limited, there is a lack of data how common it is in marbles. Our data have indicated that, in all investigated samples, which differ in the degree of bowing, residual strain could be detected. All samples have shown comparable macroscopic strain magnitudes for the *c*-axes whereas microscopic strain is most obvious perpendicular <c> of the strongest deformed sample P3. Maximum positive (dilatational) strain has been detected on the strongly deformed facade panel (P3) for the *a*-axis in the direction acquired by detector unit 8 with $\varepsilon = (980 \pm 170) \times 10^{-6}$. The strain state can be characterised by a symmetric 3×3 deformation tensor

$$\varepsilon_{kl} = 1,2,3 \quad (2)$$

The relationship between the stress and the deformation tensor is given by Hooke's law

$$\varepsilon_{kl} = \sum S_{ij,kl}\sigma_{kl} \quad (3)$$

where $S_{ij,kl}$ are the elastic compliance constants of the crystal. Conversely, the stresses σ_{kl} are given by

$$\sigma_{ij} = \sum C_{ij,kl}\varepsilon_{kl} \quad (4)$$

where $C_{ij,kl}$ are the elastic constants or stiffness coefficients. Taking into account the elastic constant $C_{a\text{-}axis}$ =87.8 GPa, the measured strain value corresponds to a residual stress magnitude of about $\sigma = (86 \pm 15)$ MPa. The maximum negative (compressive) strain value has been recorded in the good conditioned facade panel in the direction measured by detector unit 8 with $(-425 \pm 177) \times 10^{-6}$, corresponding to a compressive residual stress magnitude of $\sigma = (-37 \pm 15)$ MPa.

The measured residual strain magnitudes acquired perpendicular to the foliation plane (detector unit 8) are much higher than in the direction parallel to the foliation plane (detector unit 2). The relation of the above to the direction of the plates bowing can be recognised because the sign of bowing is 'concave' in the orientation perpendicular to the foliation plane. The observed texture is characterised by preferred orientation of the basal (0006)-planes perpendicular to the foliation plane. The strong texture of the Peccia marble is a significant evidence that the sample has experienced a deformation or the crystallographic preferred orientation is caused by thermal stress. However, further investigations of microstructural features, weathering and thermal effects are necessary for a better understanding of the bowing of marble facade panels.

Acknowledgements This work was supported through the BMBF grants 03-DUO3X4 and 03-DUO3G1. We thank the University of Göttingen for providing the deformed facade panels, K.J. Stein for the quarry sample of Peccia, and the Frank Laboratory for Neutron Physics in Dubna for providing the neutron beam to carry out the texture and strain measurements. Constructive reviews by G. Braun and K. Ullemeyer are thankfully appreciated by the authors.

References

Bortz SA, Erlin B, Monk CB (1988) Some field problems with thin veneer building stones. In: Donaldson B (ed) New stone technology, design and construction for exterior wall systems, ASTM STP 996. American Society for Testing and Materials, Philadelphia, pp 11–31

Emery CL (1964) Strain energy in rocks. In: Judd WR (ed) State of stress in the Earth crust. Elsevier, New York, pp 234–279

Franzini M (1995) Stones in monuments: natural and anthropogenic deterioration of marble artifacts. Eur J Mineral 7:735–743

Friedman M (1972) Residual elastic strain in rocks. Tectonophysics 15:297–330

Frischbutter A, Neov D, Scheffzük C, Vrána M, Walther K (2000) Lattice strain measurements on sandstones under load using neutron diffraction. J Struct Geol 22(11/12):1587–1600

Frischbutter A, Walther K, Scheffzük C (2002) Strainmessungen an geologischen Proben mit dem Diffraktometer EPSILON-MDS (Vereinigtes Institut für Kernforschung Dubna, Russische Föderation). PSI-Proceedings: Anwenderworkshop zu Spannungsfeldmessungen mittels Neutronen (Paul-Scherrer-Institut Villigen, CH):75–83

Gross KA, Paterson M (1965) Natural X-ray line broadening in limestones and marbles. Am J Sci 263:238–244

Hoskin ER, Russel JE (1981) The origin of the measured residual strains in crystalline rocks. In: Friedman M, Logan J, Stearns DW (eds) Mechanical behaviour of crustal rocks. Am Geophys Union, Washington DC 24:187–198

Kessler DW (1919) Physical and chemical tests of the commercial marbles of the United States. Technologic tests of the Bureau of Standards no 123, 54 pp.

Kleber W (1990) Einführung in die Kristallographie, Verlag Technik GmbH, Berlin

Koch A, Siegesmund S (2002) Bowing of marble panels: on-site damage analysis from the Oeconomicum Building at Göttingen (Germany). In: Siegesmund S, Weiss T, Vollbrecht A (eds) Natural stone, weathering phenomena, conservation strategies and case studies. Spec Publ Geol Soc Lond 205:299–314

Koch A, Siegesmund S (2004) The combined effect of moisture and temperature on the anomalous expansion behaviour of marble. Environ Geol (this volume) DOI 10.1007/s00254-004-1037-9

Logan JM (2004) Laboratory and case studies of thermal cycling and stored strain on the stability of selected marble. Environ Geol (this volume) DOI 10.1007/s00254-004-1047-7

Logan JM, Hadedt M, Lehnert D, Denton M (1993) A case study of the properties of marble as building veneer. Int J Rock Mech Min Sci Geomech Abstr 30(7):1531–1537

Mustonen J (1993) Finlandia-Talon julkisivujen korjaus. Rakennusinsinööri-pälvät RIL K160-1993:61–68

Nordtest Method NT BUILD 500 (2002) Cladding panels: field method for measurement of bowing. Nordtest Project 1443-99/2

Ondrasina J, Kirchner D, Siegesmund S (2002) Freeze–thaw cycles and their influence on marble deterioration: a long-term experiment. In: Siegesmund S, Weiss T, Vollbrecht A (eds)

Natural stone, weathering phenomena, conservation strategies and case studies. Spec Publ Geol Soc Lond 205:9–18
Pintschovius L (1992) Macrostresses, microstresses and stress tensors. In: Hutchings MT, Krawitz AD (eds) Measurement of residual and applied stress using neutron diffraction. Kluwer, NATO ASI Series E, no 216, Dordrecht, pp 115–130
Rayleigh Lord (1934) The bending of marble. Proc R Soc A 144:266–279
Reik G (1976) Residuelle Spannungen in quarzreichen Gesteinen: Röntgendiffraktometrische Messung und Erklärungsmöglichkeiten ihrer Entstehung. Geol Rundsch 65:66–83
Reik G, Vardar M (1974) Bestehen Zusammenhänge zwischen residuellen Spannungen und tektonischer Beanspruchung? Rock Mech 6:101–116
Ritter H (1992) Die Marmorplatten sind falsch dimensioniert. Stein 1:18–19
Sage JD (1988) Thermal microfracturing of marble. In: Marinos PG, Koukis GC (eds) Engineering geology of ancient works, monuments and historical sites. Balkema, Rotterdam, pp 1013–1018
Savage WZ (1978) The development of residual stresses in cooling rock bodies. Geophys Res Lett 5:633–636
Scheffzük Ch, Frischbutter A, Walther K (1998) Intracrystalline strain measurements with neutron diffraction: application to a Cretaceous sandstone from the Elbezone (Germany). Schriftenr Geowiss 6:39–48
Scheffzük Ch, Walther K, Frischbutter A (2001) Applied and residual strain/stress measurements on a dolomite rock sample using neutron time-of-flight diffraction. J Neutron Res 9 (2–4):187–192
Siegesmund S, Ullemeyer K, Weiss T, Tschegg EK (2000) Physical weathering of marbles caused by anisotropic thermal expansion. Int J Earth Sci 89:170–182
Timoshenko SP, Goodier JN (1970) Theory of elasticity, 3rd edn. McGraw-Hill, New York
Ullemeyer K, Spalthoff P, Heinitz J, Isakov NN, Nikitin AN, Weber K (1998) The SKAT texture diffractometer at the pulsed reactor IBR-2 at Dubna: experimental layout and first measurements. Nuclear Instr Method Phys Res A 412:80–88
Voight B (1966) Restspannungen im Gestein. Proc First Congr Int Soc Rock Mech 2:45–50
Vollbrecht A, Rust S, Weber K (1991) Development of microcracks in granites during cooling and uplift: examples from the Variscan basement in NE-Bavaria, Germany. J Struct Geol 7:787–799
Walther K, Frischbutter A, Scheffzük Ch (1998) The diffractometer Epsilon for the measurement of strains: an estimation of the full stress tensor. Schriftenr Geowiss 6:19–28
Walther K, Scheffzük C, Frischbutter A (2000) Neutron time-of-flight diffractometer Epsilon for strain measurements: layout and first results. Phys B, Condensed Matter 276–278:130–131
Walther K, Frischbutter A, Scheffzük Ch, Kenkmann T, Eichhorn F, Daymond MR (2004) Strain scanning across a shock- deformed quartzite/dunite interface. Tectonophysics (in press)
Weiss T, Siegesmund S, Fuller ER Jr (2002) Thermal stresses and microcracking in calcite and dolomite marbles via finite element modelling. In: Siegesmund S, Weiss T, Vollbrecht A (eds) Natural stone, weathering phenomena, conservation strategies and case studies. Geol Soc Spec Publ Lond 205:89–102
Weiss T, Siegesmund S, Fuller ER Jr (2003) Thermal degradation of marble: indications from finite element modelling. Building Environ 38:1251–1260
Widhalm C, Tschegg E, Eppensteiner W (1996) Anisotropic thermal expansion causes deterioration of marble cladding. J Perf Construct Facility ASCE 10:5-10
Winkler EM (1994) Stone in architecture, 3rd edn. Springer, New York
Zeisig A, Siegesmund S, Weiss T (2002) Thermal expansion and its control on the durability of marbles. In: Siegesmund S, Weiss T, Vollbrecht A (eds) Natural stone, weathering phenomena, conservation strategies and case studies. Geol Soc Spec Publ Lond 205:65–80